

Multireference configuration interaction and perturbation theory without reduced density matrices

Ankit Mahajan,^{1,*} Nick S. Blunt,² Iliya Sabzevari,¹ and Sandeep Sharma^{1,†}

¹*Department of Chemistry, University of Colorado, Boulder, CO 80302, USA*

²*Department of Chemistry, Lensfield Road, Cambridge, CB2 1EW, United Kingdom*

The computationally expensive evaluation and storage of high-rank reduced density matrices (RDMs) has been the bottleneck in the calculation of dynamic correlation for multireference wavefunctions in large active spaces. We present a stochastic formulation of multireference configuration interaction (MRCI) and perturbation theory (MRPT) that avoids the need for these expensive RDMs. The algorithm presented here is flexible enough to incorporate a wide variety of active space reference wavefunctions including selected configuration interaction, matrix product states, and symmetry-projected Jastrow mean field wavefunctions. It enjoys the usual attractive features of Monte Carlo methods such as embarrassing parallelizability and low memory costs. We find that the stochastic algorithm is already competitive with the deterministic algorithm for small active spaces containing as few as 14 orbitals. We illustrate the utility of our stochastic formulation using benchmark applications.

1. INTRODUCTION

A quantitative treatment of electronic structure in molecules that contain strongly correlated electrons has been a challenge for quantum chemical methods. It is often useful to distinguish between two flavors of electron correlation: static and dynamic. Static correlation is a result of nearly degenerate electronic states and strong interactions between them. A telltale sign of this type of correlation is the dramatic failure of single-reference methods like Hartree-Fock (HF) accompanied by divergences in Møller-Plesset perturbation theory and coupled cluster theory. Multireference (MR) methods overcome this shortcoming by treating all (or a large number of) configurations in an active space on an equal footing. The active space itself usually consists of the manifold of nearly degenerate orbitals around the Fermi surface. Examples of MR methods include full configuration interaction (FCI), density matrix renormalization group (DMRG),^{1,2} semistochastic heat bath configuration interaction (SHCI),^{3,4} full configuration interaction quantum Monte Carlo (FCIQMC),⁵⁻⁷ and their self consistent field extensions known as complete active space self consistent field (CASSCF),⁸⁻¹⁰ DMRG-SCF,¹¹⁻¹³ SHCI-SCF,¹⁴ and FCIQMC-SCF,^{15,16} respectively. While CASSCF is limited to rather small active spaces (usually less than 20 electrons and orbitals), the rest of these methods have been used in considerably larger active spaces.¹⁷⁻²⁶

Dynamic correlation is related to the fact that the wavefunction has a non-analytic cusp at the electron coalescence point, which counteracts the divergence of the Coulomb interaction. This non-analyticity is impossible to capture using a small number of smooth basis functions such as Gaussians and plane waves. Relatively large basis sets along with explicitly correlated terms which are functions of the inter-electronic distance are needed to remedy this problem. Even with the inclusion of the explicitly correlated terms, triple zeta basis sets

are often needed to obtain chemical accuracy. In multireference theories, the dynamic correlation is described by making use of methods such as perturbation theory (e.g. complete active space second order perturbation (CASPT2) theory^{27,28} and n-electron valence perturbation (NEVPT) theory),²⁹⁻³¹ configuration interaction (e.g. multireference configuration interaction (MRCI) approaches)³²⁻³⁴, multireference coupled cluster theories (MRCC),³⁵ canonical transformation (CT) theory,^{36,37} or the driven similarity renormalization group (DSRG) method.³⁸

Efficient implementations of all flavors of multireference theories that are used to capture dynamic correlation utilize internally contracted states (we will describe them in more detail in Section 2.1). The great advantage of using internally contracted states is that the cost of the calculation no longer scales exponentially with the size of the active space, however, the disadvantage is that the memory cost of the calculation is a high order polynomial of the active space size. For example, in perturbation theory and configuration interaction theory, up to fourth-order reduced density matrices in the active space are needed. The cost of storing these reduced density matrices scales as the 8th power of the number of orbitals in the active space. Although this is still manageable for small active spaces containing 20 or fewer orbitals (the limit of a CASSCF calculation), it becomes prohibitive for the large active space calculations of the type that can be performed using modern MR methods such as DMRG, FCIQMC and selected CI.³⁹⁻⁴¹ Various approaches and approximations have been proposed in the past, including (a) the use of cumulant approximation,⁴²⁻⁴⁹ (b) storing 4-RDM as batches of transition 3-RDM on disk,⁵⁰ (c) uncontracting terms that require 4-RDMs (partial contraction),^{51,52} (d) treating some terms that require 4-RDMs using matrix product states,^{53,54} and (e) performing time-propagation.⁵⁵ Each of these approaches have shortcomings, for example, the cumulant approximation is highly unstable and leads to significant intruder

state problems that can sometimes be fixed by including a level shift. Although the approaches (b) and (c) reduce the memory cost, they still require one to generate and store the 3-RDM which is quite expensive. The apparent exponential scaling of the uncontracted terms in (c) can be avoided using matrix product states perturbation theory.^{53,54,56,57} Finally, the time-dependent approach completely eliminates the need to store RDMs, but so far it has only been demonstrated to work with NEVPT2, where the special structure of the zeroth-order Dyal's Hamiltonian is used and it remains to be seen if this approach can be extended to more general perturbation theories and configuration interaction.

In this article, we present a stochastic formulation of the MRCI and NEVPT2 methods, that eliminates the need for constructing and storing the reduced density matrices. To reduce the number of parameters, we use a higher level of contraction, than the internal contraction, called strong contraction (SC).²⁹ We use an algorithm that is essentially identical to the Variational Monte Carlo (VMC) to optimize the wavefunction and calculate the energies of the SC-MRCI, and we term this approach SC-MRCI(s). This algorithm is extended to sample the Davidson size-consistency correction allowing us to calculate the SC-MRCI+Q energy up to small stochastic noise. For SC-NEVPT2(s), we again use the stochastic method to calculate the norms and energies of the perturber states, which allows us to calculate the first-order wavefunction and second-order energy corrections. The approach here is agnostic to the type of wavefunction used for performing the active space calculation and is compatible with FCI, selected CI, matrix product states, and symmetry-projected Jastrow mean field states⁵⁸⁻⁶¹.

The rest of this article is organized as follows: First, we briefly review the wavefunctions arising from the various contraction schemes and follow with the presentation of the SC-MRCI(s) and SC-NEVPT(s) algorithms. We also report details of our implementation when the FCI or selected CI methods are used to obtain the reference state. Finally, we report benchmark calculations performed using these methods, along with comparisons with the deterministic MRCI and NEVPT2 algorithms.

2. THEORY

2.1. Overview of contraction schemes

The zeroth-order wavefunction $|\phi_0\rangle$ is assumed to be an accurate representation of the exact wavefunction in the active space. It can be obtained by one of the several methods listed in the introduction, although in this work we will only be using CASSCF. Next, we begin by looking at various contraction schemes used in multireference theories to calculate dynamical correlation.

In the uncontracted methods, the wavefunction spans the entire first-order interaction space (FOIS),⁶² which

consists of all determinants that couple to the active space reference through the Hamiltonian. It is only possible to use the uncontracted scheme with relatively small systems (and active spaces). Various contraction schemes have been proposed to tackle larger systems. In the fully internally contracted (FIC)^{63,64} approach, single and double excitation operators are directly applied to $|\phi_0\rangle$ instead of individual determinants, resulting in a more compact wavefunction given by

$$|\psi_{\text{FIC}}\rangle = c_0|\phi_0\rangle + \sum_{p,a} c_p^a a_a^\dagger a_p |\phi_0\rangle + \sum_{p,q,a,b} c_{pq}^{ab} a_a^\dagger a_b^\dagger a_p a_q |\phi_0\rangle + \sum_{p,q,r,s} c_{pq}^{rs} a_r^\dagger a_s^\dagger a_p a_q |\phi_0\rangle, \quad (1)$$

where a, b, \dots denote virtual orbitals, while p, q, \dots denote internal (core and active) ones. Notice that the number of parameters in the FIC scheme is at most quartic in the size of the active space, unlike the uncontracted scheme where it is exponential. Despite the enormous reduction in the number of parameters, the FIC results are usually in very good agreement with those of the uncontracted methods. One drawback of the FIC scheme relative to the uncontracted wavefunction is that the internally contracted states ($a_a^\dagger a_b^\dagger a_p a_q |\phi_0\rangle$) are no longer orthogonal, which often leads to ill-conditioned generalized eigenvalue problems and in most algorithms, this difficulty is overcome by explicitly diagonalizing the overlap matrix and eliminating the zero-eigenvectors. The strong contraction (SC) approximation alleviates the non-orthogonality problem by further contracting the subspaces through Hamiltonian matrix elements. Here, we follow the notation introduced by Malrieu *et al.*²⁹ Let $S_l^{(k)}$ denote the subspace of FIC-FOIS, where k is the change in the number of active electrons ($-2 \leq k \leq 2$) and l denotes the configuration of electrons in the core and virtual spaces. In the SC theory, only a single state $|\psi_l^{(k)}\rangle$ from each $S_l^{(k)}$ is used. Specifically,

$$|\psi_l^{(k)}\rangle = P_l^{(k)} H |\phi_0\rangle, \quad (2)$$

where $P_l^{(k)}$ is the projector onto the $S_l^{(k)}$ space. Equivalently, this state is obtained by eliminating the active indices of the FIC states by contracting with the one and two electron integrals. For example, the following state from the $S_{ab}^{(-2)}$ subspace is used:

$$|\psi_{ab}^{(-2)}\rangle = \sum_{pq} (\langle ab|pq\rangle - \langle ab|qp\rangle) a_a^\dagger a_b^\dagger a_p a_q |\phi_0\rangle. \quad (3)$$

An exception to this rule is made for the $S_0^{(0)}$ space, which is represented by the state $|\phi_0\rangle$. Implicit in this simplification is the assumption that $|\phi_0\rangle$ is the eigenstate of the active space Hamiltonian (H_0), otherwise an additional term $H_0|\phi_0\rangle$ should also be included. Using these states the SC wavefunction is described as

$$|\psi_{\text{SC}}\rangle = \sum_{k,l} c_l^{(k)} |\psi_l^{(k)}\rangle.$$

Note that the states $|\psi_l^{(k)}\rangle$ are mutually orthogonal (although not normalized).

Neese *et al.* have argued that using the SC approximation doesn't lead to a large gain in efficiency in the deterministic MRCI algorithm.⁶⁵ In our stochastic formulation, we found the SC approximation to lead to a much easier optimization problem. It is also known to allay intruder state problems in perturbation theory. Thus we will focus on the SC methods below.

2.2. SC-MRCI(s)

In this section, we outline the use of the SC-MRCI wavefunction as a VMC ansatz and its optimization using our improved orbital space VMC algorithm. In VMC, the energy of a wavefunction $|\psi(\mathbf{p})\rangle$, where \mathbf{p} is the set of parameters, can be computed using importance sampling as

$$\begin{aligned} \frac{\langle \psi(\mathbf{p}) | H | \psi(\mathbf{p}) \rangle}{\langle \psi(\mathbf{p}) | \psi(\mathbf{p}) \rangle} &= \sum_n \frac{|\langle n | \psi(\mathbf{p}) \rangle|^2}{\langle \psi(\mathbf{p}) | \psi(\mathbf{p}) \rangle} \frac{\langle n | H | \psi(\mathbf{p}) \rangle}{\langle n | \psi(\mathbf{p}) \rangle} \\ &= \left\langle \frac{\langle n | H | \psi(\mathbf{p}) \rangle}{\langle n | \psi(\mathbf{p}) \rangle} \right\rangle_{\rho_n}, \end{aligned} \quad (4)$$

where $|n\rangle$ is a Slater determinant walker, $\rho_n = \frac{|\langle n | \psi(\mathbf{p}) \rangle|^2}{\langle \psi(\mathbf{p}) | \psi(\mathbf{p}) \rangle}$ is the probability distribution used for Monte Carlo sampling. The quantity sampled is called local energy, given by

$$E_L[n] = \frac{\langle n | H | \psi(\mathbf{p}) \rangle}{\langle n | \psi(\mathbf{p}) \rangle} = \sum_n \langle n | H | m \rangle \frac{\langle m | \psi(\mathbf{p}) \rangle}{\langle n | \psi(\mathbf{p}) \rangle}. \quad (5)$$

For an efficient calculation of local energy, it is essential to be able to calculate the walker overlap ratios $\left(\frac{\langle m | \psi(\mathbf{p}) \rangle}{\langle n | \psi(\mathbf{p}) \rangle}\right)$ appearing in the above equations efficiently.

Let's look at these overlaps carefully for the SC-MRCI wavefunction. Note that each walker belongs to a unique $S_l^{(k)}$ subspace. We will denote the subspace a walker $|n\rangle$ belongs to by $S_{l_n}^{(k_n)}$. Thus the overlap of the walker with a general contracted state is given by

$$\langle n | \psi_l^{(k)} \rangle = \begin{cases} \delta_{k,0} \delta_{l,0} \langle n | \phi_0 \rangle, & \text{if } |n\rangle \in S_0^{(0)}, \\ \delta_{k,k_n} \delta_{l,l_n} \langle n | H | \phi_0 \rangle, & \text{if } |n\rangle \notin S_0^{(0)}. \end{cases} \quad (6)$$

The overlap of the walker with $|\psi_{\text{SC}}\rangle$ is given by

$$\langle n | \psi_{\text{SC}} \rangle = c_{l_n}^{(k_n)} \langle n | \psi_{l_n}^{(k_n)} \rangle. \quad (7)$$

As $|\phi_0\rangle$ is assumed to be a selected CI wavefunction, its overlap with a walker can be calculated in $O(1)$ time by storing the determinants and coefficients in a hash table. We note that the local energy calculation is feasible for any wavefunction that allows efficient evaluation of these overlaps.

The walkers are sampled from the probability distribution ρ_n by using the rejection free continuous time Monte Carlo (CTMC) algorithm,^{66,67} the details of which can be seen in Ref. 68. All quantities required for CTMC sampling are calculated and stored during the local energy evaluation at no additional cost.

We now turn to the problem of optimizing the wavefunction parameters, which in this case are the CI coefficients. At first glance, it would appear that analogous to the deterministic algorithms, the linear method^{69–72} should be able to optimize this linearly parametrized wavefunction in a single step. While this is true in theory, the linear method becomes very expensive for a large number of parameters both in terms of time and memory cost.^{73,74} In our experiments, we have found that it can only be feasibly applied when the number of coefficients is less than about 50,000. Since the number of states in an MRCI wavefunction often exceeds this number, the linear method does not appear to be a suitable choice in this problem. We instead choose AMSGrad, an accelerated stochastic gradient method developed in the machine learning community.⁷⁵ Its utility in wavefunction optimization in VMC has recently been reported.^{61,68,76,77} It should be noted that SGD has been used implicitly to solve CI problems in FCIQMC and its many variants.⁷⁶ AMSGrad requires an estimate of the energy gradient, which can be sampled as

$$\mathbf{g}_i = \frac{\partial E}{\partial p_i} = \left\langle \frac{\langle \psi_i(\mathbf{p}) | n \rangle}{\langle \psi(\mathbf{p}) | n \rangle} (E_L(n) - E) \right\rangle_{\rho_n}, \quad (8)$$

where $|\psi_i(\mathbf{p})\rangle = \left| \frac{\partial \psi(\mathbf{p})}{\partial p_i} \right\rangle$ is the wavefunction derivative and E is the energy of the wavefunction. For $|\psi_{\text{SC}}\rangle$ the wavefunction derivative overlaps are given by

$$\langle n | \psi_{k,l} \rangle = \delta_{k,k_n} \delta_{l,l_n} \langle n | \psi_l^{(k)} \rangle, \quad (9)$$

where $|\psi_{k,l}\rangle$ denotes the derivative with respect to $c_l^{(k)}$. These quantities are needed for local energy calculation (Equation 6) and are thus easily obtained.

The Davidson size-consistency correction is given by

$$\Delta_D E = (1 - a_0^2)(E_{\text{SC-MRCI}} - E_0^{(0)}), \quad (10)$$

where a_0 is the coefficient of the normalized reference in the normalized SC-MRCI wavefunction. a_0 is not entirely trivial to obtain because we don't explicitly know the norm of each of the SC states. Instead, we calculate a_0^2 by first noting that

$$a_0^2 = \frac{\langle \phi_0 | \psi_{\text{opt}} \rangle^2}{\langle \phi_0 | \phi_0 \rangle \langle \psi_{\text{opt}} | \psi_{\text{opt}} \rangle} = \left(c_0^{(0)} \right)^2 \frac{\langle \phi_0 | \phi_0 \rangle}{\langle \psi_{\text{opt}} | \psi_{\text{opt}} \rangle}, \quad (11)$$

where $|\psi_{\text{opt}}\rangle$ is the optimized SC-MRCI wavefunction and $c_0^{(0)}$ is the (known) coefficient of $|\phi_0\rangle$ in this wavefunction. The ratio of overlaps

$$\begin{aligned} \frac{\langle \phi_0 | \phi_0 \rangle}{\langle \psi_{\text{opt}} | \psi_{\text{opt}} \rangle} &= \sum_n \frac{|\langle n | \psi_{\text{opt}} \rangle|^2}{\langle \psi_{\text{opt}} | \psi_{\text{opt}} \rangle} \frac{|\langle n | \phi_0 \rangle|^2}{|\langle n | \psi_{\text{opt}} \rangle|^2} \\ &= \langle \delta_{k_n,0} \delta_{l,0} \rangle_{\rho_n} \end{aligned} \quad (12)$$

can be calculated using the CTMC algorithm, which when multiplied by $(c_0^{(0)})^2$ gives us the value of a_0^2 needed to calculate the Davidson size-consistency correction.

2.3. SC-NEVPT2(s)

The SC-NEVPT2 first-order correction is given by

$$|\psi^{(1)}\rangle = \sum_{k,l \neq 0} \frac{1}{E_0^{(0)} - E_l^{(k)}} |\psi_l^{(k)}\rangle, \quad (13)$$

where, the perturber state energies $E_l^{(k)}$ are defined as

$$E_l^{(k)} = \frac{\langle \psi_l^{(k)} | H_D | \psi_l^{(k)} \rangle}{\langle \psi_l^{(k)} | \psi_l^{(k)} \rangle}. \quad (14)$$

And the second order SC-NEVPT2 energy correction is given by

$$E^{(2)} = \sum_{k,l \neq 0} \frac{1}{E_0^{(0)} - E_l^{(k)}} \frac{\langle \psi_l^{(k)} | \psi_l^{(k)} \rangle}{\langle \psi_0^{(0)} | \psi_0^{(0)} \rangle}, \quad (15)$$

In Eq. 14, H_D is Dyall's Hamiltonian,⁷⁸ the zeroth-order Hamiltonian employed in NEVPT. It is defined as

$$H_D = \sum_i^{\text{core}} \epsilon_i a_i^\dagger a_i + \sum_a^{\text{virtual}} \epsilon_a a_a^\dagger a_a + H_0,$$

where i and a denote the orbitals obtained by diagonalizing the core and virtual generalized Fock operators, respectively, and ϵ_i and ϵ_a the corresponding eigenenergies. H_0 is the full core-averaged Hamiltonian in the active space.

The energies $E_l^{(k)}$ can be obtained using Monte Carlo sampling of the numerator and denominator separately

$$\begin{aligned} \frac{\langle \psi_l^{(k)} | H_D | \psi_l^{(k)} \rangle}{\langle \psi_s | \psi_s \rangle} &= \sum_n \frac{|\langle n | \psi_s \rangle|^2 \langle \psi_l^{(k)} | n \rangle \langle n | H_D | \psi_l^{(k)} \rangle}{\langle \psi_s | \psi_s \rangle \langle \psi_s | n \rangle \langle n | \psi_s \rangle}, \\ \frac{\langle \psi_l^{(k)} | \psi_l^{(k)} \rangle}{\langle \psi_s | \psi_s \rangle} &= \sum_n \frac{|\langle n | \psi_s \rangle|^2 |\langle \psi_l^{(k)} | n \rangle|^2}{\langle \psi_s | \psi_s \rangle |\langle \psi_s | n \rangle|^2}. \end{aligned} \quad (16)$$

where, $|\psi_s\rangle$ wavefunction is used for importance sampling. In our calculations we use the sampling wavefunction is given by

$$|\psi_s\rangle = \sum_{k,l} c_l^{(k)} |\psi_l^{(k)}\rangle, \quad (17)$$

where we choose the coefficients $c_l^{(k)}$ randomly, with the condition that $c_0^{(0)}$ is about an order of magnitude bigger than other coefficients. In principle, it is sufficient to choose any state $|\psi_s\rangle$ that has a non-zero overlap with all

the perturber states $|\psi_l^{(k)}\rangle$. The quantities in Eq. 16 for all classes $S_l^{(k)}$ are sampled together using a single CTMC run similar to the one used for SC-MRCI(s) calculations. Note that the square norm ratios required for calculating the second-order energy correction (cf. Eq. 15) are also obtained in the same sampling run. In our experience, calculating the energy correction requires more sampling effort than calculating the coefficients in the wavefunction correction, likely because the variance of the quantities sampled to estimate the norms of the SC states is higher. Some perturber states have a small norm, which can be of the same order as the stochastic noise. This can cause numerical instabilities because the norms appear in the denominator of Eq. 14. To avoid this the perturber states with a small norm are screened out. The screening does not cause significant error in the SC-NEVPT2 energies because the norm appears in the numerator of Eq. 15.

2.4. Implementation

We have implemented these algorithms for selected CI reference wavefunctions with core electrons uncorrelated. Consider the expression for local energy given in Eq. 5:

$$E_L[n] = \sum_n \langle n | H | m \rangle \frac{\langle m | \psi(\mathbf{p}) \rangle}{\langle n | \psi(\mathbf{p}) \rangle}.$$

The walker $|n\rangle$ belongs to either the CAS or the FOIS. The determinants $|m\rangle$ are generated from $|n\rangle$ through the Hamiltonian. Note that only those $|m\rangle$'s that are at most doubly excited from the CAS have a non-zero overlap with the wavefunction and thus only these excitations need to be generated. If the resulting $|m\rangle$ is not in the CAS, we again need to generate excitations from this determinant using the Hamiltonian to calculate its overlap with the wavefunction (cf. Eq. 6). The number of determinants that need to be generated from $|m\rangle$ is significantly less than the number of all determinants connected to it since they have to be in the CAS to have a non-zero overlap with $|\phi_0\rangle$. We use the heat-bath algorithm³ to generate all excitations efficiently. The determinants in the reference $|\phi_0\rangle$ are stored in a hash table, so the overlap of a determinant with it can be calculated in constant time on average. Because this method avoids calculation of the expensive RDMs, its memory cost is negligible compared to the deterministic algorithm. Similar considerations apply to the quantities sampled in SC-NEVPT2(s), with the exception that in this case, the first set of excitations are generated using Dyall's Hamiltonian instead of the full system Hamiltonian. This implementation can be extended to correlate core electrons and to work with other kinds of reference wavefunctions.

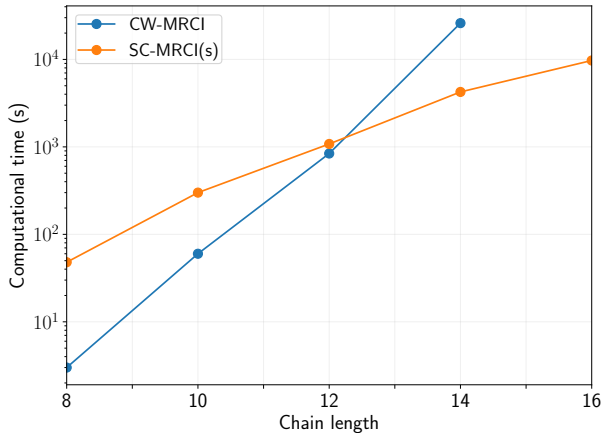


FIG. 1. Computational time in seconds for CW-MRCI and SC-MRCI(s) calculations of hydrogen chains H_n in the 6-31g basis set using the (ne, no) active space consisting of all 1s orbitals. The CW-MRCI calculations were performed serially while the SC-MRCI(s) calculations were performed using 24 cores.

3. RESULTS

In this section, we will present some applications of SC-MRCI(s) and SC-NEVPT2(s) with a selected CI reference to demonstrate its utility in treating multireference problems quantitatively. We compare all our energies to Celani-Werner (CW) MRCI energies obtained using MOLPRO,⁷⁹ version 2019.1. We used PySCF⁸⁰ to generate Hamiltonian integrals and to obtain the CASSCF wavefunction. Selected CI program Dice^{3,4,14} was used to obtain the important determinants in the CASSCF wavefunction. In all calculations, we retained enough determinants in the selected CI wavefunction to get an energy within $0.2 mE_h$ of the CASSCF energy.

We report the computational timings for SC-MRCI(s) calculations of hydrogen chains of increasing length and compare them with CW-MRCI. We also present the potential energy curve for N_2 and analyze the efficacy of the Davidson correction for achieving approximate size-consistency.

3.1. Hydrogen chain

We calculated MRCI energies of open hydrogen chains of increasing lengths in the 6-31g basis set. The bond length was set to 2 Bohr in all calculations. The active space consisting of the 1s orbitals on each hydrogen was used. Fig. 4 shows the computational times, and Table 1 shows the ground state energies for SC-MRCI(s) and CW-MRCI.

AMSGrad was used to optimize the variational energy and to obtain the converged SC-MRCI(s) wavefunction.

TABLE 1. Ground state energies (E_h) for hydrogen chains H_n in the 6-31g basis set. Stochastic errors in the QMC calculations are less than $1 mE_h$.

Chain length	CW-MRCI	SC-MRCI(s)
8	-4.416	-4.415
10	-5.518	-5.516
12	-6.620	-6.618
14	-7.722	-7.719
16	-	-8.820

It usually requires fewer iterations to converge to the final result if more stochastic samples are used. In our numerical experiments, we have found that using enough samples to obtain energies with an error of $\sim 10 mE_h$ in the first iteration leads to smooth optimization in most cases. 2400 stochastic samples were enough to achieve this accuracy for all chain lengths considered here. We progressively increased the number of stochastic samples as the wavefunction approached convergence, and all the reported SC-MRCI(s) energies here have a stochastic error of less than $1 mE_h$. Calculations were performed on a single compute node with two Intel[®] Xeon[®] E5-2680 v3 processors (2.5 GHz) and 116 GB memory. SC-MRCI(s) calculations were parallelized over all available cores using MPI, while MOLPRO calculations were performed serially since a parallel implementation is not available. It is apparent from Fig. 1 that although CW-MRCI is very efficient for smaller active spaces, its scaling with the size of the active space is worse compared to SC-MRCI(s). This can be attributed to the use of uncontracted excitations for certain semi-internal excitation classes in CW-MRCI. As a result, for even the moderately sized H_{14} chain, SC-MRCI(s) achieves a performance similar to CW-MRCI. For the H_{16} chain, we were unable to perform the CW-MRCI calculation on a single node, while the SC-MRCI(s) calculation took only about three hours. We note that CW-MRCI can be parallelized to obtain better performance but not as effectively as VMC, which is embarrassingly parallelizable. The timings for SC-MRCI(s) can be reduced linearly by using more processors thus offsetting the larger prefactor often present in the scaling of VMC methods. For this small basis set, the absolute differences in energies between the two methods are relatively small, with the SC approximation leading to errors of less than $3 mE_h$. Based on this evidence, we can say that SC-MRCI(s) can be feasibly scaled to larger active spaces by using reference wavefunctions such as symmetry projected Jastrow mean-field, matrix product states, etc. With some improvement in the implementation, the stochastic algorithm might compare much more favorably relative to the deterministic methods for even small to moderate-sized active spaces.

TABLE 2. Results for N_2 in the cc-pVTZ basis set. The CW-MRCI+Q column shows the ground state energies in E_h , while the other columns show differences from CW-MRCI+Q in mE_h . Stochastic errors in the CI methods are less than 1 mE_h . The (10e, 8o) active space with frozen 1s orbitals was used in all calculations. The last row shows nonparallelity errors with respect to the CW-MRCI+Q results in mE_h .

d (Bohr)	CW-MRCI+Q	CW-MRCI	SC-MRCI(s)	SC-MRCI+Q(s)	SC-NEVPT2(s)
1.8	-109.285	12	18	8	40
2.2	-109.367	13	19	7	40
2.5	-109.301	14	19	8	40
3.0	-109.171	15	21	8	41
3.6	-109.074	17	21	7	42
4.2	-109.042	16	20	6	42
5.0	-109.033	15	18	4	41
\parallel error		5	3	4	3

3.2. N_2

We calculated the ground state potential energy curve of N_2 in the cc-pVTZ basis. The (10e,8o) active space consisting of the 2s and 2p electrons and orbitals was used. The 1s core electrons were frozen in all calculations. The results are shown in Table 2. We used 48,000 stochastic samples in all SC-MRCI(s) calculations for each AMSGrad iteration, and a final single point calculation with enough stochastic samples to achieve an error less than 1 mE_h was performed whenever necessary. We have found that the number of stochastic samples needed to obtain a given accuracy scales roughly linearly with the number of variables in the wavefunction.

For SC-NEVPT2(s) calculations, 1,120,000 stochastic samples were used. The greater number of stochastic samples was needed partly because the second-order correction to the energy is a non-linear function of $E_l^{(k)}$ (see Eq. 15), which is itself calculated stochastically. As a result, in addition to a stochastic error, the SC-NEVPT2(s) energy also has a systematic bias, as has been investigated in other QMC methods previously.^{81,82} However, with the relatively large number of stochastic samples used here, we find that the systematic bias is smaller than the stochastic noise. We confirmed this by ensuring that the energy didn't change by more than $1mE_h$ when more stochastic samples were used. We also compared the SC-NEVPT2(s) energies to those obtained deterministically using MOLPRO and found good agreement between the two.

SC-MRCI+Q(s) gives energies closest to CW-MRCI+Dav. and has a nonparallelity error of 4 mE_h . Despite having the largest absolute errors, SC-NEVPT2(s) has the smallest nonparallelity error of 3 mE_h . The SC approximation leads to larger absolute errors in MRCI compared to NEVPT2. Nonetheless, the nonparallelity errors in both theories due to the SC approximation are remarkably small. We note that SC-MRCI results of similar quality have also been reported in Refs. 65 and 83.

Table 3 shows the size-consistency errors for these methods. All stochastic CI energies, in this case, were converged to an accuracy of 0.5 mE_h . SC-NEVPT2(s) is

exactly size consistent (within stochastic error) as expected. CW-MRCI and SC-MRCI(s) have large size-consistency errors which arise due to the same reasons as in the single-reference CI case. The Davidson correction does seem to remedy this issue to a large extent. The relatively small nonparallelity and size-consistency errors in the SC-MRCI+Q(s) and SC-NEVPT2(s) methods are encouraging and indicate that it may be feasible to treat problems with a large number of virtual orbitals using our framework.

TABLE 3. Size-consistency errors for N_2 calculated as the difference between the energy of two well separated atoms and twice the energy of a single atom.

Method	ΔE (mE_h)
SC-NEVPT2(s)	0.0
CW-MRCI	7.6
CW-MRCI+Q	1.0
SC-MRCI(s)	8.0
SC-MRCI+Q(s)	2.1

4. CONCLUSIONS

In this work, we have presented stochastic formulations of SC-MRCI and SC-NEVPT2 methods that do away with the requirement of storing expensive high-order active space RDMs. The need to calculate and store these RDMs has been a major bottleneck in calculating dynamic correlation in multireference theories, especially when active spaces are large. Using benchmark calculations on hydrogen chains and the nitrogen molecule, we have argued that the stochastic method, presented here, represents an attractive alternative to the deterministic methods. It outperforms the corresponding deterministic method even with active spaces that are as small as 14 orbitals.

Our work also highlights the accuracy of the strongly contracted wavefunctions, which is in agreement with the work done previously. However, even with this relatively small loss of accuracy, the use of strong contraction in deterministic algorithms is often not recommended be-

cause the saving in computational time relative to internal or partial contraction is negligible. This metric drastically changes in the stochastic approach presented here because the optimization problem one needs to solve when using strong contraction is significantly easier than when partial or internal contraction is used. Thus with stochastic methods, our recommendation is to use strong contraction and only resort to internal contraction when it is known that the former is likely to fail.

This work will be extended in several directions. All calculations presented here have used the frozen core approximation. We are working on an efficient implementation of excitation classes that correlate core electrons. It will be interesting to see how the stochastic method performs with other reference wavefunctions such as matrix product states, symmetry projected Jastrow mean-field, etc. A problem that we have not discussed here is that the strongly contracted wavefunctions are not invariant to unitary transformations in the virtual orbitals. Our preliminary results indicate that the results are most accurate when canonical CASSCF virtual orbitals are used, however, the efficiency of calculation suffers when such delocalized orbitals are used. More work is needed to determine what kind of virtual (and core) orbitals will lead to the “best” results. The fact that our formulation can be used with many different active-space wavefunctions and places virtually no restrictions on the size of the active or virtual spaces, raises the exciting prospect of performing multireference calculations on large systems that are beyond the reach of current methodologies.

5. ACKNOWLEDGEMENTS

The funding for this project was provided by the national science foundation through the grant CHE-1800584. SS was also partly supported through the Sloan research fellowship. NSB is grateful to St John’s College, Cambridge for funding through a Research Fellowship.

REFERENCES

* ankitmahajan76@gmail.com

† sanshar@gmail.com

- ¹ White, S. R.; Martin, R. L. Ab initio quantum chemistry using the density matrix renormalization group. *The Journal of chemical physics* **1999**, *110*, 4127–4130.
- ² Chan, G. K.-L.; Sharma, S. The density matrix renormalization group in quantum chemistry. *Annual review of physical chemistry* **2011**, *62*, 465–481.
- ³ Holmes, A. A.; Tubman, N. M.; Umrigar, C. J. Heat-Bath Configuration Interaction: An Efficient Selected Configuration Interaction Algorithm Inspired by Heat-Bath Sampling. *J. Chem. Theory Comput.* **2016**, *12*, 3674–3680, PMID: 27428771.
- ⁴ Sharma, S.; Holmes, A. A.; Jeanmairet, G.; Alavi, A.; Umrigar, C. J. Semistochastic Heat-bath Configuration Interaction method: selected configuration interaction with semistochastic perturbation theory. *J. Chem. Theory Comput.* **2017**, *13*, 1595–1604.
- ⁵ Booth, G. H.; Thom, A. J. W.; Alavi, A. Fermion Monte Carlo without fixed nodes: A game of life, death, and annihilation in Slater determinant space. *J. Chem. Phys.* **2009**, *131*, 054106.
- ⁶ Cleland, D.; Booth, G. H.; Alavi, A. Communications: Survival of the fittest: Accelerating convergence in full configuration-interaction quantum Monte Carlo. *J. Chem. Phys.* **2010**, *132*, 041103.
- ⁷ Petruzielo, F. R.; Holmes, A. A.; Changlani, H. J.; Nightingale, M. P.; Umrigar, C. J. Semistochastic Projector Monte Carlo Method. *Phys. Rev. Lett.* **2012**, *109*, 230201.
- ⁸ Roos, B. O.; Taylor, P. R.; Si, P. E., et al. A complete active space SCF method (CASSCF) using a density matrix formulated super-CI approach. *Chemical Physics* **1980**, *48*, 157–173.
- ⁹ Roos, B. O. The complete active space SCF method in a fock-matrix-based super-CI formulation. *International Journal of Quantum Chemistry* **1980**, *18*, 175–189.
- ¹⁰ Siegbahn, P. E.; Almlöf, J.; Heiberg, A.; Roos, B. O. The complete active space SCF (CASSCF) method in a Newton–Raphson formulation with application to the HNO molecule. *The Journal of Chemical Physics* **1981**, *74*, 2384–2396.
- ¹¹ Ghosh, D.; Hachmann, J.; Yanai, T.; Chan, G. K.-L. Orbital optimization in the density matrix renormalization group, with applications to polyenes and β -carotene. *The Journal of chemical physics* **2008**, *128*, 144117.
- ¹² Zgid, D.; Nooijen, M. The density matrix renormalization group self-consistent field method: Orbital optimization with the density matrix renormalization group method in the active space. *The Journal of chemical physics* **2008**, *128*, 144116.
- ¹³ Yanai, T.; Kurashige, Y.; Ghosh, D.; Chan, G. K.-L. Accelerating convergence in iterative solution for large-scale complete active space self-consistent-field calculations. *International Journal of Quantum Chemistry* **2009**, *109*, 2178–2190.
- ¹⁴ Smith, J. E.; Mussard, B.; Holmes, A. A.; Sharma, S. Cheap and near exact CASSCF with large active spaces. *J. Chem. Theory Comput.* **2017**, *13*, 5468–5478.
- ¹⁵ Thomas, R. E.; Sun, Q.; Alavi, A.; Booth, G. H. Stochastic Multiconfigurational Self-Consistent Field Theory. *J. Chem. Theory Comput.* **2015**, *11*, 5316.
- ¹⁶ Li Manni, G.; Smart, S. D.; Alavi, A. Combining the complete active space self-consistent field method and the full configuration interaction quantum Monte Carlo within a super-CI framework, with application to challenging metal-porphyrins. *Journal of chemical theory and computation* **2016**, *12*, 1245–1258.
- ¹⁷ Hachmann, J.; Dorando, J. J.; Avilés, M.; Chan, G. K.-L. The radical character of the acenes: A density matrix renormalization group study. *The Journal of chemical physics* **2007**, *127*, 134309.
- ¹⁸ Marti, K. H.; Ondřík, I. M.; Moritz, G.; Reiher, M. Density matrix renormalization group calculations on relative energies of transition metal complexes and clusters. *The Journal of chemical physics* **2008**, *128*, 014104.
- ¹⁹ Kurashige, Y.; Yanai, T. High-performance ab initio density matrix renormalization group method: Applicability to large-scale multireference problems for metal compounds. *The Journal of chemical physics* **2009**, *130*, 234114.

- ²⁰ Kurashige, Y.; Chan, G. K.-L.; Yanai, T. Entangled quantum electronic wavefunctions of the Mn 4 CaO 5 cluster in photosystem II. *Nature chemistry* **2013**, *5*, 660.
- ²¹ Sharma, S.; Sivalingam, K.; Neese, F.; Chan, G. K.-L. Low-energy spectrum of iron-sulfur clusters directly from many-particle quantum mechanics. *Nature chemistry* **2014**, *6*, 927.
- ²² Olivares-Amaya, R.; Hu, W.; Nakatani, N.; Sharma, S.; Yang, J.; Chan, G. K.-L. The ab-initio density matrix renormalization group in practice. *The Journal of chemical physics* **2015**, *142*, 034102.
- ²³ Mussard, B.; Sharma, S. One-Step Treatment of Spin-Orbit Coupling and Electron Correlation in Large Active Spaces. *Journal of chemical theory and computation* **2017**, *14*, 154-165.
- ²⁴ Li, J.; Otten, M.; Holmes, A. A.; Sharma, S.; Umrigar, C. J. Fast semistochastic heat-bath configuration interaction. *J. Chem. Phys.* **2018**, *149*, 214110.
- ²⁵ Booth, G. H.; Grüneis, A.; Kresse, G.; Alavi, A. Towards an exact description of electronic wavefunctions in real solids. *Nature* **2013**, *493*, 365.
- ²⁶ Li Manni, G.; Alavi, A. Understanding the mechanism stabilizing intermediate spin states in Fe (II)-porphyrin. *The Journal of Physical Chemistry A* **2018**, *122*, 4935-4947.
- ²⁷ Andersson, K.; Malmqvist, P. A.; Roos, B. O.; Sadlej, A. J.; Wolinski, K. Second-order perturbation theory with a CASSCF reference function. *Journal of Physical Chemistry* **1990**, *94*, 5483-5488.
- ²⁸ Andersson, K.; Malmqvist, P.-Å.; Roos, B. O. Second-order perturbation theory with a complete active space self-consistent field reference function. *The Journal of chemical physics* **1992**, *96*, 1218-1226.
- ²⁹ Angeli, C.; Cimiraglia, R.; Evangelisti, S.; Leininger, T.; Malrieu, J.-P. Introduction of n-electron valence states for multireference perturbation theory. *The Journal of Chemical Physics* **2001**, *114*, 10252-10264.
- ³⁰ Angeli, C.; Cimiraglia, R.; Malrieu, J.-P. n-electron valence state perturbation theory: A spinless formulation and an efficient implementation of the strongly contracted and of the partially contracted variants. *The Journal of chemical physics* **2002**, *117*, 9138-9153.
- ³¹ Angeli, C.; Borini, S.; Cestari, M.; Cimiraglia, R. A quasidegenerate formulation of the second order n-electron valence state perturbation theory approach. *The Journal of chemical physics* **2004**, *121*, 4043-4049.
- ³² Werner, H.-J.; Knowles, P. J. An efficient internally contracted multiconfiguration-reference configuration interaction method. *The Journal of chemical physics* **1988**, *89*, 5803-5814.
- ³³ Knowles, P. J.; Werner, H.-J. An efficient method for the evaluation of coupling coefficients in configuration interaction calculations. *Chemical physics letters* **1988**, *145*, 514-522.
- ³⁴ Knowles, P. J.; Werner, H.-J. Internally contracted multiconfiguration-reference configuration interaction calculations for excited states. *Theoretica chimica acta* **1992**, *84*, 95-103.
- ³⁵ Bartlett, R. J.; Musial, M. Coupled-cluster theory in quantum chemistry. *Reviews of Modern Physics* **2007**, *79*, 291.
- ³⁶ Yanai, T.; Chan, G. K.-L. Canonical transformation theory for multireference problems. *The Journal of chemical physics* **2006**, *124*, 194106.
- ³⁷ Neuscammann, E.; Yanai, T.; Chan, G. K.-L. A review of canonical transformation theory. *International Reviews in Physical Chemistry* **2010**, *29*, 231-271.
- ³⁸ Evangelista, F. A. A driven similarity renormalization group approach to quantum many-body problems. *The Journal of chemical physics* **2014**, *141*, 054109.
- ³⁹ Kurashige, Y.; Yanai, T. Second-order perturbation theory with a density matrix renormalization group self-consistent field reference function: Theory and application to the study of chromium dimer. *The Journal of chemical physics* **2011**, *135*, 094104.
- ⁴⁰ Guo, S.; Watson, M. A.; Hu, W.; Sun, Q.; Chan, G. K.-L. N-electron valence state perturbation theory based on a density matrix renormalization group reference function, with applications to the chromium dimer and a trimer model of poly (p-phenylenevinylene). *Journal of chemical theory and computation* **2016**, *12*, 1583-1591.
- ⁴¹ Roemelt, M.; Guo, S.; Chan, G. K.-L. A projected approximation to strongly contracted N-electron valence perturbation theory for DMRG wavefunctions. *The Journal of chemical physics* **2016**, *144*, 204113.
- ⁴² Zgid, D.; Ghosh, D.; Neuscammann, E.; Chan, G. K.-L. A study of cumulant approximations to n-electron valence multireference perturbation theory. *The Journal of chemical physics* **2009**, *130*, 194107.
- ⁴³ Saitow, M.; Kurashige, Y.; Yanai, T. Multireference configuration interaction theory using cumulant reconstruction with internal contraction of density matrix renormalization group wave function. *The Journal of chemical physics* **2013**, *139*, 044118.
- ⁴⁴ Kurashige, Y.; Chalupský, J.; Lan, T. N.; Yanai, T. Complete active space second-order perturbation theory with cumulant approximation for extended active-space wavefunction from density matrix renormalization group. *The Journal of chemical physics* **2014**, *141*, 174111.
- ⁴⁵ Saitow, M.; Kurashige, Y.; Yanai, T. Fully internally contracted multireference configuration interaction theory using density matrix renormalization group: A reduced-scaling implementation derived by computer-aided tensor factorization. *Journal of chemical theory and computation* **2015**, *11*, 5120-5131.
- ⁴⁶ Shirai, S.; Kurashige, Y.; Yanai, T. Computational evidence of inversion of 1La and 1Lb-derived excited states in naphthalene excimer formation from ab Initio multireference theory with large active space: DMRG-CASPT2 Study. *Journal of chemical theory and computation* **2016**, *12*, 2366-2372.
- ⁴⁷ Phung, Q. M.; Wouters, S.; Pierloot, K. Cumulant approximated second-Order perturbation theory based on the density matrix renormalization group for transition metal complexes: a benchmark study. *Journal of chemical theory and computation* **2016**, *12*, 4352-4361.
- ⁴⁸ Yanai, T.; Saitow, M.; Xiong, X.-G.; Chalupsk, J.; Kurashige, Y.; Guo, S.; Sharma, S. Multistate Complete-Active-Space Second-Order Perturbation Theory Based on Density Matrix Renormalization Group Reference States. *Journal of chemical theory and computation* **2017**, *13*, 4829-4840.
- ⁴⁹ Nakatani, N.; Guo, S. Density matrix renormalization group (DMRG) method as a common tool for large active-space CASSCF/CASPT2 calculations. *The Journal of Chemical Physics* **2017**, *146*, 094102.
- ⁵⁰ Wouters, S.; Van Speybroeck, V.; Van Neck, D. DMRG-CASPT2 study of the longitudinal static second hyperpolarizability of all-trans polyenes. *The Journal of chemical physics* **2016**, *145*, 054120.

- ⁵¹ Celani, P.; Werner, H.-J. Multireference perturbation theory for large restricted and selected active space reference wave functions. *J. Chem. Phys.* **2000**, *112*, 5546–5557.
- ⁵² Shamasundar, K.; Knizia, G.; Werner, H.-J. A new internally contracted multi-reference configuration interaction method. *The Journal of chemical physics* **2011**, *135*, 054101.
- ⁵³ Sharma, S.; Chan, G. K.-L. Communication: A flexible multi-reference perturbation theory by minimizing the Hylleraas functional with matrix product states. 2014.
- ⁵⁴ Sharma, S.; Knizia, G.; Guo, S.; Alavi, A. Combining internally contracted states and matrix product states to perform multireference perturbation theory. *Journal of chemical theory and computation* **2017**, *13*, 488–498.
- ⁵⁵ Sokolov, A. Y.; Guo, S.; Ronca, E.; Chan, G. K.-L. Time-dependent N-electron valence perturbation theory with matrix product state reference wavefunctions for large active spaces and basis sets: Applications to the chromium dimer and all-trans polyenes. *The Journal of chemical physics* **2017**, *146*, 244102.
- ⁵⁶ Sharma, S.; Alavi, A. Multireference linearized coupled cluster theory for strongly correlated systems using matrix product states. *The Journal of chemical physics* **2015**, *143*, 102815.
- ⁵⁷ Sharma, S.; Jeanmairet, G.; Alavi, A. Quasi-degenerate perturbation theory using matrix product states. *The Journal of chemical physics* **2016**, *144*, 034103.
- ⁵⁸ Tahara, D.; Imada, M. Variational Monte Carlo method combined with quantum-number projection and multi-variable optimization. *J. Phys. Soc. Jpn.* **2008**, *77*, 114701.
- ⁵⁹ Neuscamman, E. Size consistency error in the antisymmetric geminal power wave function can be completely removed. *Phys. Rev. Lett.* **2012**, *109*, 203001.
- ⁶⁰ Neuscamman, E. The Jastrow antisymmetric geminal power in Hilbert space: Theory, benchmarking, and application to a novel transition state. *J. Chem. Phys.* **2013**, *139*, 194105.
- ⁶¹ Mahajan, A.; Sharma, S. Symmetry-Projected Jastrow Mean-Field Wave Function in Variational Monte Carlo. *The Journal of Physical Chemistry A* **2019**, *123*, 3911–3921.
- ⁶² McLean, A.; Liu, B. Classification of configurations and the determination of interacting and noninteracting spaces in configuration interaction. *The Journal of Chemical Physics* **1973**, *58*, 1066–1078.
- ⁶³ Meyer, W. *Modern Theoretical Chemistry*; Plenum Press New York, 1977.
- ⁶⁴ Siegbahn, P. E. Direct configuration interaction with a reference state composed of many reference configurations. *International Journal of Quantum Chemistry* **1980**, *18*, 1229–1242.
- ⁶⁵ Sivalingam, K.; Krupicka, M.; Auer, A. A.; Neese, F. Comparison of fully internally and strongly contracted multireference configuration interaction procedures. *The Journal of chemical physics* **2016**, *145*, 054104.
- ⁶⁶ Bortz, A.; Kalos, M.; Lebowitz, J. A new algorithm for Monte Carlo simulation of Ising spin systems. *J. Comput. Phys.* **1975**, *17*, 10 – 18.
- ⁶⁷ Gillespie, D. T. A general method for numerically simulating the stochastic time evolution of coupled chemical reactions. *J. Comp. Phys.* **1976**, *22*, 403 – 434.
- ⁶⁸ Sabzevari, I.; Sharma, S. Improved Speed and Scaling in Orbital Space Variational Monte Carlo. *J. Chem. Theory Comput.* **2018**, *14*, 6276–6286.
- ⁶⁹ Nightingale, M.; Melik-Alaverdian, V. Optimization of ground-and excited-state wave functions and van der Waals clusters. *Physical review letters* **2001**, *87*, 043401.
- ⁷⁰ Umrigar, C.; Toulouse, J.; Filippi, C.; Sorella, S.; Hennig, R. G. Alleviation of the fermion-sign problem by optimization of many-body wave functions. *Physical review letters* **2007**, *98*, 110201.
- ⁷¹ Toulouse, J.; Umrigar, C. J. Optimization of quantum Monte Carlo wave functions by energy minimization. *The Journal of chemical physics* **2007**, *126*, 084102.
- ⁷² Toulouse, J.; Umrigar, C. Full optimization of Jastrow–Slater wave functions with application to the first-row atoms and homonuclear diatomic molecules. *The Journal of chemical physics* **2008**, *128*, 174101.
- ⁷³ Zhao, L.; Neuscamman, E. A blocked linear method for optimizing large parameter sets in variational monte carlo. *Journal of chemical theory and computation* **2017**, *13*, 2604–2611.
- ⁷⁴ Sabzevari, I.; Mahajan, A.; Sharma, S. An accelerated linear method for optimizing non-linear wavefunctions in variational Monte Carlo. *arXiv preprint arXiv:1908.04423* **2019**,
- ⁷⁵ Reddi, S. J.; Kale, S.; Kumar, S. On the Convergence of Adam and Beyond. International Conference on Learning Representations. 2018; pp 1–23.
- ⁷⁶ Schwarz, L. R.; Alavi, A.; Booth, G. H. Projector Quantum Monte Carlo Method for Nonlinear Wave Functions. *Physical review letters* **2017**, *118*, 176403.
- ⁷⁷ Otis, L.; Neuscamman, E. Complementary First and Second Derivative Methods for Ansatz Optimization in Variational Monte Carlo. *Physical Chemistry Chemical Physics* **2019**,
- ⁷⁸ Dyall, K. G. The choice of a zeroth-order Hamiltonian for second-order perturbation theory with a complete active space self-consistent-field reference function. *The Journal of chemical physics* **1995**, *102*, 4909–4918.
- ⁷⁹ Werner, H.-J.; Knowles, P. J.; Knizia, G.; Manby, F. R.; Schütz, M. Molpro: a general-purpose quantum chemistry program package. *WIREs Comput. Mol. Sci.* **2012**, *2*, 242–253.
- ⁸⁰ Sun, Q.; Berkelbach, T. C.; Blunt, N. S.; Booth, G. H.; Guo, S.; Li, Z.; Liu, J.; McClain, J. D.; Sayfutyarova, E. R.; Sharma, S.; Wouters, S.; Chan, K.-L. G. PySCF: the Python-based simulations of chemistry framework. *WIREs Comput. Mol. Sci.* **2018**, *8*, e1340.
- ⁸¹ Zhao, L.; Neuscamman, E. Equation of Motion Theory for Excited States in Variational Monte Carlo and the Jastrow Antisymmetric Geminal Power in Hilbert Space. *Journal of Chemical Theory and Computation* **2016**, *12*, 3719–3726.
- ⁸² Blunt, N. S.; Alavi, A.; Booth, G. H. Nonlinear biases, stochastically sampled effective Hamiltonians, and spectral functions in quantum Monte Carlo methods. *Physical Review B* **2018**, *98*, 085118.
- ⁸³ Angeli, C.; Cimiraglia, R.; Pastore, M. A comparison of various approaches in internally contracted multireference configuration interaction: the carbon dimer as a test case. *Molecular Physics* **2012**, *110*, 2963–2968.